

Implications of lithium-ion cell temperature estimation methods for intelligent battery management and fast charging systems

Ahmed Abd EL BASET Abd EL HALIM¹ ^{*}, Ehab Hassan EID BAYOUMI², Walid EL-KHATTAM³,
and Amr Mohamed IBRAHIM³

¹ Energy and Renewable Energy Department, Faculty of Engineering, Egyptian Chinese University, 14 Abou Ghazalh, Mansheya El-Tahrir, Ain Shams, Cairo, Egypt

² Department of Mechanical Engineering, Faculty of Engineering, The British University in Egypt, El Sherouk City, Cairo, Egypt

³ Department of Electric Power and Machines, Faculty of Engineering, Ain Shams University, Cairo, Egypt

Abstract. This article examines in depth the most recent thermal testing techniques for lithium-ion batteries (LIBs). Temperature estimation circuits can be divided into six divisions based on modeling and calculation methods, including electrochemical computational modeling, equivalent electric circuit modeling (EECM), machine learning (ML), digital analysis, direct impedance measurement and magnetic nanoparticles as a base. Complexity, accuracy and computational cost-based EECM circuits are feasible. The accuracy, usability and adaptability of diagrams produced using ML have the potential to be very high. However, none of them can anticipate the low-cost integrated BMS in real time due to their high computational costs. An appropriate solution might be a hybrid strategy that combines EECM and ML.

Keywords: BMS; fast charging; lithium-ion batteries; machine learning; thermal testing techniques.

1. INTRODUCTION

Due to their high voltage (> 4 V/cell), high energy density (265 (Wh) L^{-1}) and longer lifespan, LIBs are frequently employed in electric vehicles (EVs), reliable grid-connected energy storage systems and various other consumer gadgets. The usage of LIBs in the transportation and aerospace sectors has resulted in more giant cells and battery packs with longer ranges and more demanding charge and discharge cycles. However, thermal instability and temperature-dependent nonlinear behavior frequently hampered LIB systems' safe and dependable functioning. The performance of the Li-ion battery, including its longevity, efficiency, dependability and safety, is directly impacted by using the battery outside of its safe operating temperature. The ideal working temperature range for LIBs, according to studies on their thermal efficiency, is between 25°C and 40°C [1, 2]. According to [3], profound charging circumstances and varied charging current requirements can cause the internal temperature and surface temperature to diverge by more than 10°C in real applications. Thermal shock, explosion and fire can result from excessive temperature difference and high-temperature concentration inside the battery [4]. In order to properly monitor battery parameters (current, voltage and temperature) and evaluate battery health (state of charge (SOC), state of health (SOH), remaining usable life (RUL), and state of

temperature (SOT) [5]), a battery management system (BMS) is required. Studies have demonstrated that SOC [6], SOH [7] and residual storage capacity [8] are functions of temperature; as a result, the temperature of a battery during charging and discharging has a significant impact on the Coulombic efficiency of the battery. Other standard BMS functions include cell balancing [9] and fault detection/diagnosis [10], which frequently require knowledge of cell and individual cell temperatures for optimal energy usage, operational safety, reliability and long battery life.

As a result, accurate core and surface temperature knowledge is crucial for effective thermal control and security of LIB cells. Heating the battery to the proper limits to ensure adequate performance at low temperatures can also drastically diminish battery capacity in areas with a cold climate [11, 12]. Additionally, research has revealed that the battery deteriorates by about 5% for every 0.1°C increase outside of the safe operating range [13, 14]. According to the research, the discharge process – particularly the rapid discharge process – is when most of the heat is emitted. Therefore, accurate temperature estimation is crucial for good thermal management and safety when the battery is quickly depleted and heated to prevent energy loss.

For LIBs thermal management and safety, precise battery temperature information is unquestionably a crucial cornerstone. Although each cell can have a temperature sensor placed inside of it to monitor the surface temperature, it is challenging to use a physical probe to measure the inside temperature directly. The thousands of batteries and modules contained within each high-capacity battery used in EVs and grid-connected systems make it

*e-mail: ahmedabdelbaset2016@gmail.com

Manuscript submitted 2023-05-31, revised 2023-05-31, initially accepted for publication 2024-01-16, published in May 2024.

impractical to install temperature sensors on every surface of the battery. This has an impact on system cost, footprint and weight. To create an intelligent battery, researchers have also combined multi-dimensional (MD) sensing and self-healing capabilities into a single battery [15–18]. Intelligent batteries measure variables and evaluate the battery's health, including temperature. Accurate temperature estimation is still required in intelligent batteries despite the modular deployment of BMS, as placing sensors in each cell would increase operational expenses and complexity. To create a low-cost car BMS, researchers tried to create a highly accurate, exact, easy-to-implement and computationally cheap online temperature estimating algorithm. To measure temperature, academics have come up with several different approaches thus far.

Regarding the above-mentioned qualities of an ideal BMS, each of the various types of techniques has its benefits and drawbacks. To choose the best technology for a given need, researchers and developers can benefit greatly from having a broad overview of all currently used technologies as a starting point for further investigation. However, there needs to be a synopsis of the literature that outlines the developments and explains the present issues, difficulties and potential for further study. This work covers this research gap by thoroughly examining the most recent temperature-estimating techniques published in the literature.

2. GENERIC TEMPERATURE ESTIMATION STRATEGY

Regardless of the battery's chemistry, heat is generated inside the battery during charge/discharge cycles and while it is at rest. This heat is generated through chemical, electrochemical and predominantly exothermic transport processes. Insufficient heat flow from the battery to the surroundings can cause heat to accumulate inside the battery, raising internal and surface temperatures and the possibility of thermal shock. Batteries with rigid insulation, which are utilized in EVs and have quick charge/discharge rates and high operating temperatures, are the ones where this effect is most visible. Heat conductivity of cylindrical lithium batteries, frequently utilized in big lithium batteries, could be more substantial. So, exothermic and heat transport

models make up a standard heat estimating system [19]. While other models use mathematical forms of battery chemistry to compute heat generation, the Bernard heat generation model (HGM) [20] is also used typically to estimate the total heat produced. Battery temperature is a function of the battery condition, so the adaptation algorithm also considers the effects of different battery conditions, such as SOC and SOH. The predicted total temperature is then used to anticipate battery temperature using a heat transfer model (HTM) and additional outside measurements, e.g. ambient temperature. Measured or estimated temperature is used as feedback in feedback scoring systems to increase forecast accuracy. Figure 1 depicts a schematic representation of a general LIB temperature evaluation scheme.

3. CLASSIFICATION OF TES

A temperature estimation system typically comprises a heat release model and HTM, as shown in Fig. 1. Heat source-based approaches and modeling can be used to broadly categorize the heat release patterns that have been described in the literature. Three types of simulation strategy-based heating models may be identified: EECM [22, 23], physics-based electrochemical models [24–27], and black-box models [28–30]. According to various heat sources, these models can be divided into centralized, distributed models [31] and heterogeneous models [25, 32]. Geothermal models typically assume that all heat is produced solely in the core, which is assumed to simplify the simulation. While heterogeneity models capture variable heat generation in distinct cell layers, frequently leading to temperature and current density within the cell, diffusion heating models provide for homogenous heating across the cell shape.

Heterogeneous models are the most complex ones and require a great deal of modeling expertise, but they are also most detailed and may provide very accurate forecasts. Between centralized and heterogeneous models, the distributed heating model strikes a balance. Thermal resistance models (coupled or dispersed variables) [27, 33–36], finite element analysis (FEM) models [28, 37–40] and data-based techniques are three categories of HTMs. The capacitive-resistive thermal model uses an analogy between electrical and thermal systems. Thermistor

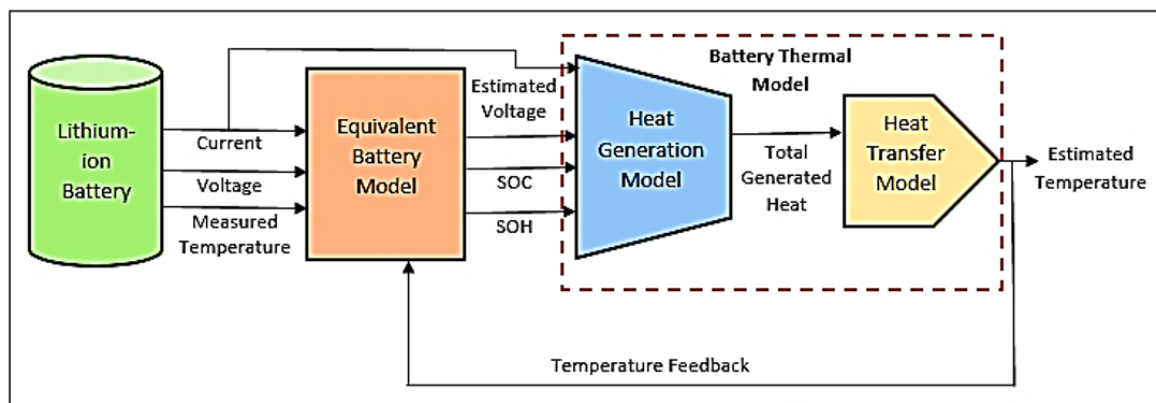


Fig. 1. Schematic layout of a generic temperature estimation strategy (TES) for a LIB cell [21]

Implications of lithium-ion cell temperature estimation methods for intelligent battery management and fast charging systems

resistors can be categorized into several groups, as shown in Fig. 2. Coupled parameter models are straightforward and appropriate for grid systems. However, they can only forecast one or two average temperatures, and the distribution of the battery in space is not uniform, particularly for cylindrical lithium batteries with higher capacities. However, due to the difficulty of the calculations, sophisticated distributed models [41, 42] are not appropriate for networks even though they can precisely explain temperature distribution within cells. Other intricate LIB models have been researched [43–48], considering the thermal characteristics of many layers. One-state/node models only provide information on the core temperature, whereas the two-state model (TSM)/two-node model provides core and surface temperatures.

Battery heating models are a subset of HTMs that accept the total amount of heat produced as an input variable and estimate

the total heat produced by the batteries. To create an estimated heat system, researchers used a variety of heat-generating models and HTMs. Since LIB thermal modeling is a separate area of research, it is not included in this investigation. It only addresses the policy of temperature ratings. Most TES, however, strongly rely on thermal modeling; thus, for better comprehension, this page gives a brief description of each modeling technique and the accompanying TES.

Consequently, it is challenging to classify various evaluation techniques. Electrochemical, thermal modeling-based systems, EECM-based systems, ML-based systems, numerical modeling-based systems, direct resistivity measurement-based systems and magnetic nanoparticles-based systems are the main categories of temperature estimation programs. Figure 2 displays the LIB series’ thermal model, heat transmission model, and method for estimating temperature.

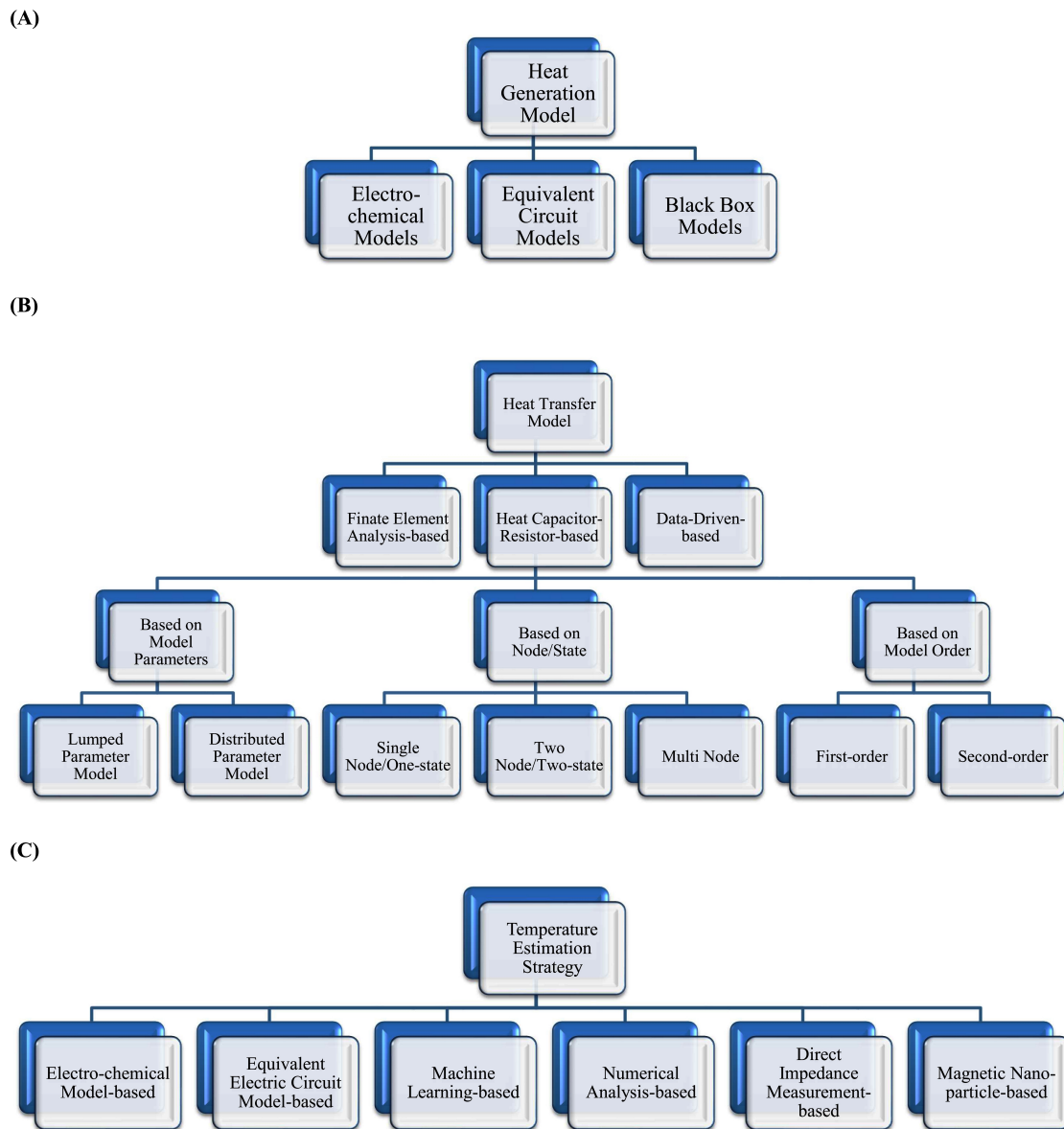


Fig. 2. Model series for: (A) HGM, (B) HTM, (C) TES [21]

4. METHODS FOR ESTIMATING TEMP.

4.1. Electrochemical thermal modeling-based system

To simulate battery temperatures under various operating situations, geometries or cooling rates, researchers started developing thermal modeling in the early 1990s. These models were frequently integrated with electrochemical models. They ranged from straightforward 1D (radial) models to intricate three-dimensional (3D) thermal models [37, 49–59]. To create mathematical models of the electrochemical behavior of batteries, scientists primarily use various analytical techniques. In one-dimensional (1D) models, isothermal flow and the battery's thermophysical characteristics are assumed to have constant heat release rates.

To account for temperature fluctuations brought on by ohmic resistance, chemical reactions, mixing processes, polarization and electrical resistance, very complicated 3D models necessitate in-depth knowledge of the thermodynamic properties of battery materials and components, i.e. electrode kinetics. Very intricate models can be used to estimate temperature with a high degree of accuracy, but these precise models are crucial for battery construction. They are incompatible with low computing resource BMS temperature estimation. These sophisticated models can explain how batteries' nonlinear behavior changes over time. However, they frequently call for different system characteristics and operating settings, which necessitate significant experimental testing. However, other characteristics, such as those related to transport, thermodynamics and thermal impacts, are very challenging to assess.

To calculate the overall heat dissipation during charge/discharge, [60] devised a comprehensive LIB heat dissipation model based on electrochemical simulations. Thomas and Newman's basic equation for a LIB's overall temperature is:

$$Q = I(V - U^{\text{avg}}) + IT \frac{\partial U^{\text{avg}}}{\partial T} - \sum_i \Delta H_i^{\text{avg}} r_i - \int \sum_j \left(\overline{H}_j - \overline{H}_j^{\text{avg}} \right) \frac{\partial C_j}{\partial t} dv. \quad (1)$$

In (1), Q stands for the battery's heating or heat consumption rate, V and U stand for the battery's equilibrium voltage and potential, respectively, I for the charge or discharge current, and T for the battery's temperature. H_i is the reaction's change in enthalpy, and r_i is its rate. The particle concentration is c_j , and H_j is the partial molar mass of the j -th particle. The symbols for time and cell volume are t and v , respectively. Using a "responsible" index, all attributes are based on volume average concentration. While this study did not include temperature estimations, the model can only provide detailed information on temperature. Many other scientists frequently utilize this thermal model. However, due to the high number of calculations required by the simulation's level of realism, it is complicated and unsuitable for online applications.

The Doyle-Fuller-Newman model [37, 61], a popular electrochemical model, is frequently quoted and utilized in thermal modeling. The internal characteristics of a lithium-ion battery are described by a set of algebraic equations that are partially nonlinear. A different name for this is synthetic pseudo-two-

dimensional (P2D) modeling. This model's primary flaw is its heavy processing requirement, which restricts its capacity to evaluate the state of a car BMS network. A basic 1D local thermal model is sufficient for battery design, particularly for large-scale modeling of LIB thermal models, as demonstrated by [53]. Additionally, it does not thoroughly grasp how different battery parts – such as electrodes, electrolytes and separators – affect heat generation.

Few researchers have investigated pulse power limiting used to prevent thermal shock and create thermal management systems using such intricate electrochemical models [62, 63]. They are mostly employed in the creation of LIB batteries and cells. A coupled local electrochemical-thermal model is applied to forecast LIB thermal properties and specific electrode properties at various operating temperatures [64]. The model only offers outcomes from lab tests, not real-world usage scenarios, and is validated based on experimental data of a stationary hybrid vehicle (HEV) and impulse response. [65] investigated how the charging current impacted the interior temperature. To create an MD electrochemical, thermal model of LIBs that allowed for a more thorough investigation of thermal properties and thermal conductivity, [66] combined more comprehensive data and battery parameters. The models' complexity and processing cost prevent them from being applied outside of the BMS, despite the accuracy of the estimates. Not all heat sources are often modeled or taken into consideration due to the absence of a thorough understanding of the electrochemical processes occurring in LIBs and the accompanying mathematical equations to decrease the computing cost. Big mistakes in temperature estimates can result from this non-replicable heating activity. [67] created a two-site thermal model without prior information on thermal parameters using discrete and inverse modeling techniques. It is not necessary to heat model each heat source because the model can predict the overall heat produced by battery cells. Instead, aberrant heating can be identified using the results. Extra heat and fast-loading circumstances verify the model's validity and dependability. Although this method was created for self-heating batteries, it might also be used with other lithium-ion battery types. Therefore, an additional study is advised in this case. High-accuracy electrochemical models and integrated measurements like voltage and current were used by [68] to calculate battery temperature during charge/discharge at various C rates. Additionally, to relate terminal voltage to cell temperature and Li^+ concentration, they employed a dual ensemble Kalman filter (DEKF), combining individual events' extended dynamics. Accurate lithium (Li^+) concentration determination is challenging due to computationally expensive models and model complexity. Therefore, it is debatable whether to apply this model to actual network predictions. [69] used a dual de-aromatic soft-narrow Kalman filter and P2D electrochemical model to approximate the spatial distribution of temperature in LIBs (DUKF). The cost of simulation and calculation is very high, and its primary purpose is to estimate Li^+ concentration. The technique can be expanded to estimate temperature, however. A 1D spatial electrochemical-thermal model was created by [62] to investigate LIB cells' pulse power restriction and thermal behavior. Table 1 provides rapid access to the temperature estimating tech-

niques based on the electrochemical-thermal model proposed by various authors. Any model-based electrochemical technique generally has two key drawbacks: simulation complexity and high computational cost, which renders these models unsuitable for online prediction and low-cost airborne BMS.

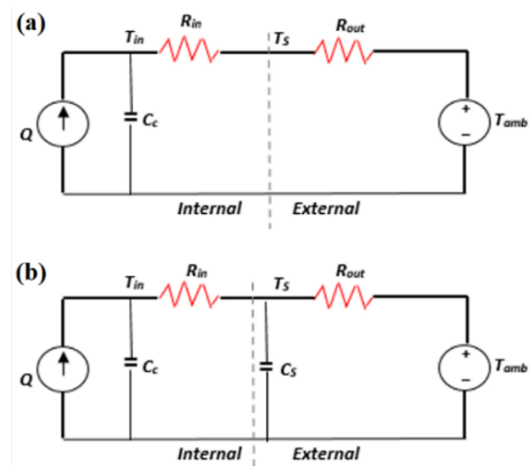
Table 1

Summary of electrochemical-thermal modeling-based TES

Model	Synopsis
Electrochemical model with only 1D [60]	Not used to estimate temperature.
P2D model [37, 61]	Used by several other studies but not for temperature estimation.
Transient 1D thermal model with lumped parameters (LP) [53]	Specific information about the electrodes, electrolytes and separator was considered in the heat generation mode.
LP electrochemical-thermal coupled model [64]	It can estimate one or two average temperatures, performs well for each electrode at different operating temperatures and considers characteristics of constant current and pulsing situations.
Thermal energy generation model, multiphase micro-macroscopic electrochemical model [41]	Temperature-dependent. Varied charging settings, physicochemical characteristics and thermal behaviors were considered. Numerical simulations, the volume-averaging technique, and the ability to estimate the average cell temperature and temperature distribution inside a cell.
1D thermal model [42]	The thermal influence of various model parameters on various discharge patterns was evaluated using simulation and experiment data.
Two-dimensional modeling + Finite element method (FEM) [65]	With the aid of MATLAB and the results of experiments and simulations, it is possible to generate temperature distribution based on potential and current density distribution.
MD electrochemical-thermal model [66]	Each cell layer's thermal characteristics are considered and empirically verified.
High-fidelity electrochemical model + onboard measurements + dual ensemble Kalman filter (DEKF) [68]	Wide range of C-rates during the charging and discharging time, validated in MATLAB using results from simulations and experiments.
P2D electrochemical model and soft-constrained dual unscented Kalman filter (DUKF) [69]	MATLAB simulation can provide details regarding the spatial distribution of internal temperature.
1D electrochemical lumped thermal model [62]	Adaptable to various drive cycles; empirically verified, tested and validated using FUDS and HWFET drive cycles.

4.2. EECM-based TES

Using power system characteristics to create a thermal battery model based on capacitors and resistors, an EECM captures LIB thermal behavior. First-order and second-order models (SOM) are the two categories of models that have been established in the literature based on the number of heat sinks (number of energy storage elements). The thermal energy storage component forms part of the first-order model (FOM). The second-order thermal model also contains two heat sinks, typically one for the battery's core heat capacity and one for the surface [13]. SOM can attain more momentum than first-order ones. Figures 3a and 3b represent thermal models of first-order and second-order LIB batteries, respectively. In Fig. 3, Q represents the rate of heat release, C_c and C_s are the respective heat capacities of the cell and surface, and T_{in} and T_{out} are ambient temperatures of the cell and surface T_{amb} 's temperatures.

**Fig. 3.** LIB cell thermal model for: (a) FOM, (b) SOM

Additionally, EECM can be further broken down into local and distributed models, depending on the intricacy of the modeling. For reasons of simplicity, LP models are more efficient computationally than comprehensive sparse models. While some studies use battery surface and core temperatures to generate local thermal models, computationally efficient local thermal models have been developed utilizing a single temperature as input to obtain model parameters [70]. Some have also used thermal modeling to examine the connection between battery shape and other physical characteristics [71]. In contrast to accurate temperature calculations, several assumptions made throughout the simulation resulted in erroneous temperature predictions.

Additionally, a thermal model that can predict both surface and core temperatures is referred to as a TSM temperature/node [67], as opposed to a model that can only predict core temperature [72]. Various experimental studies, such as electrochemical impedance spectroscopy (EIS), or outside measurements, such as voltage, current and temperature, are used to determine the EECM characteristics.

To strengthen the models, some research also considered various SOC, SOH and predicted surface/core temperature scenarios. Cluster models are utilized for one-state and TSM simulations, and the models might be first or second order, making it

challenging to categorize these thermal models. As a result, the literature is split between systems for estimating temperature at the cell- and packet levels, as explained below.

In general, these EECM models determine Q values using equation (2) proposed by [20].

$$Q = I(V - V_{ocv}) + IT_c \frac{dV_{ocv}}{dT_c}, \quad (2)$$

V_{ocv} is the battery's open circuit voltage, and $\frac{dV_{ocv}}{dT_c}$ denotes the entropy coefficient. Finally, T_c and T_s are calculated using the thermal model's mathematical representation illustrated in Fig. 3. (3) and (2) provide the mathematical equations for estimating temperature using first- and second-order thermal models (4).

4.2.1. EECM-based cell TES

Any EECM-based strategy has its share of issues, and the variable identification model is one of them. To raise the internal temperature, [43] built a local heating model. They used a short test to ascertain the model's parameters, including heat transfer coefficient and capacity. In this investigation, a 2 Hz current pulse was employed to raise the interior temperature while determining parameters using EIS. The surface temperature recorded by a local temperature model is used to estimate T_c . Entropy changes are also considered in the simulations. Figure 3a, which they created, is a first-order thermal model. [43] presented a first-order mathematical formulation of the thermal model.

$$T_{in} = T_s \left(1 + \frac{R_{in}}{R_{out}} \right) - T_{amb} \frac{R_{in}}{R_{out}}. \quad (3)$$

There needs to be a quantitative investigation of [43] strategy's impact on temperature. Compared to the extremely low currents utilized in EIS, the operational current is significantly higher. Therefore, a whole thermodynamics study cannot be performed using the model parameters generated by EIS. They also assumed a constant internal temperature; however, the same investigation found that the battery's internal spaces varied by more than 10°C in this respect. This method makes a scale inefficient since it necessitates inserting a temperature sensor into each cell to measure the surface temperature. To shorten the design process and lower the price of battery packs, [73] created a thermal model of a portable LIB in order to better understand thermal behavior under various operating situations. They demonstrate that whereas the temperature rise during discharge is primarily influenced by the heat produced inside the LIB battery, the temperature rise during charging is primarily influenced by the thermal conductivity of the electronics. Designing an effective thermal management system for LIB batteries should consider these linked factors, especially for fast charging that prioritizes health. Using KF, [13] created a second-order thermal model for a system that estimates the core's temperature. Here, the battery's thermal performance is calculated using the least squares (LS) algorithm. Although straightforward and precise, the modeling technique does not account for environmental uncertainty. Simulation-based findings and fundamental low-current discharge curves for model validation are also presented, indicating that more study is needed to ensure accuracy

for real-world applications. The models have previously undergone testing with straightforward current curves for charging and discharging.

However, the actual load curves deviate significantly from these short load curves. Therefore, two primary conductivity cycle experiments covering the range of SOC 25–100%, temperature of 5–38°C, and C-line max. etc., were used to validate the second-order LIB cylindrical cell thermal model and the two-position EECM thermal model. This C-rate is 22 [74] in humans. [74] investigated how changes in temperature and SOC affected EECM parameters and how they affected battery thermal performance. The model's predictions are reliable and accurate. Testing has not, however, been done using the global reference standard driving cycles. Therefore, more research is needed to determine the actual scenarios' accuracy and dependability. [75] discussed the effects of aging and heat transfer circumstances on thermophysical model parameters because battery aging influences EECM characteristics. [75] uses the forgetting factor recursive least squares (FFRLS) technique to alter the augmented model online.

The study by [45, 76] raises questions concerning the validity of the findings and the impact of battery aging on network deployment. The popular LS technique adapts the model to battery aging and other uncertainties and adds a novel non-uniform forgetting factor to monitor time-varying internal parameters. Due to the significant geographical and temporal temperature distribution, [77] only uses two lumped models to simulate internal and surface temperature, which might not be appropriate for large LIBs. Only a rough estimate of the battery core temperature is given because of entropy changes on heating. In order to estimate solely the interior temperature, [78] created a second-order temperature model using LP (one state). Using an EECM-based heat dissipation model, they numerically modeled the overall heat accumulation produced in the battery core. This study, which is an upgrade over earlier research, looks at the impact of entropy modifications and improvements on battery thermal performance and conducts a quantitative analysis to create software for online internal temperature estimation. When loading and unloading, this approach estimates the ambient temperature using surface and ambient temperatures, and KF is utilized for adaptive estimation with a quick real-time update procedure. On the accuracy of temperature estimation, [79] studied the effects of unmeasured simulation errors, initialization mistakes and external thermal factors that could change over time. This study created a second-order cluster thermal model for adaptive core temperature prediction based on KF. This model is depicted in Fig. 3b. Additionally, the network's internal temperature and time-varying external thermal resistance are estimated simultaneously using a single Kalman filter (JKF). Mathematical formula (4) [79] can be used to express the interior temperature as an estimate:

$$T_{in}(s) = \frac{\left(1 + \frac{R_{in}}{R_{out}} + C_S R_{in} s \right)}{C_S C_c s^2 + \left(C_s + C_c + \frac{R_{in} C_c}{R_{out}} \right) s + \frac{1}{R_{out}}} Q(s), \quad (4)$$

where s is the Laplace operator and other parameters are the same as in Fig. 3.

[79] study's accuracy increased by creating distinct thermal models for the battery's core and shell and accounting for how the external heat transfer coefficient changes over time. A portion of the temperature model was also tuned using the LS algorithm based on experimental data. The proposed method's computational efficiency is all that the authors mention; however, they do not detail the hardware or computing time needed. Additionally, the simulation makes some assumptions that result in incorrect estimations for real applications.

A compromise between LP technique and detailed thermal modeling was considered by [80] and [71]. To forecast the surface and core temperatures of LIBs, they created a two-state thermal model. The new objective is to reduce the computational cost while providing more information than the pooling parameter models. Reduced-order model (ROM) is also known as lumped by particular academics. Even though the fundamental goal is the same, it is to simplify a complex thermal problem with many thermal parameters into a more straightforward heat transfer problem. Using a joint 2RC (second order) ECCM and a core and surface temperature estimate scheme based on a joint Kalman filter, [72] suggested a combined two-site thermal model (JKF). To ensure that the model is adequate for accounting for variations in temperature and SOC, simulations and experimental tests are run. Finally, the prediction's correctness is also assessed. Additionally, it is demonstrated that the suggested model outperforms the EECM stated above in terms of prediction accuracy. The model also demonstrates excellent resistance to the automated surface thermal conductivity correction.

[81] created a 1D (radial) parametric thermal model with two Kalman filters to learn more about heat dissipation in a cylindrical LIB (DCF). The model can also give data on the temperatures at three separate battery sites based solely on core and surface temperatures. The three-node thermal model is the name given by the researchers for this simulation. To increase the precision and dependability of the forecast, this study additionally considered the anisotropy of heat conduction when determining internal resistance and SOC in the temperature estimating procedure. Different relevant payment and payment conditions' effects are not taken into consideration. Additionally, a 1 RC ECCM heating model was considered, suggesting that a 2 RC ECCM heating model would further boost accuracy. [35] used particle swarm optimization to estimate online parameters for pulse discharge studies at various ambient temperatures. To obtain more precise temperatures in a large prismatic LIB, a 2RC ECCM was integrated with a multi-site heat transfer model based on cell shape in this study. According to studies, hybrid models can achieve outcomes comparable to those of the finite element method (FEM) while utilizing around 90% fewer calculations. Additionally, it was discovered that battery geometry significantly influenced battery temperature. This study created a case-level thermal model and was highly accurate, although it ignored the impacts of battery aging.

LIB thermal model includes radiation's impact on cell surfaces on heat conduction [82]. The internal temperature is then calculated using an extended unscented Kalman filter (EUKF) that considers radiation's effects using a spatial temperature model. A new condition called sensor offset is incorporated to increase model robustness and prediction accuracy. Although

load scenarios for domestic energy storage have been evaluated, it has yet to be determined whether they are suitable for commercial vehicles. Additionally, the model's parameters are taken for granted to remain constant in environmental uncertainty, which may not be the case if the operational environment changes dramatically. To predict surface and core temperatures by considering the thermal effects of nearby cells during simulation, [83] devised a two-stage thermoelectric model. The simulation model also incorporates an extended state observer (ESO) with surface temperature feedback to account for model error and time-varying parameters. This technique was created specifically for quickly heating self-heating batteries. The idea of a virtual model-based thermal sensor (VTS) was first proposed by [84]. It consisted of a thermal model adjusted using a KF observer, an online parameter determination technique. A single temperature sensor input is used to estimate surface and core temperatures. This technique still requires sensor feedback to account for environmental unpredictability, but it cannot be deemed wholly useless. Although this lessens the need for sensors and enhances model fit, the idea is the same as that of other EECM-based approaches that use LP. Using a combination of the ECCM 1-RC, singlet thermal model and KF to estimate core temperature, [14] demonstrated the impact of fast discharge on LIB core temperature. They used an iterative least squares (RLS) approach to determine the model's thermal parameters. However, more study is advised to create a reliable BMS suitable for quick charge/discharge.

4.2.2. EECM-based TES of LIB pack

Most studies only provide a single battery's estimated temperature. Rarely are LIB battery thermal modeling and thermal estimation described. Using the LIB package ROM, which considers the battery's internal resistance characteristics, [85] carried out core temperature estimation. Here, temperature parameters are determined using RLS. Several assumptions were made when building the ROM battery to ensure that each battery's specifications and the thermal behavior of each series of batteries were the same for this investigation. Because heat transfer between the wires and bulging cells is not considered, temperature estimation can be inaccurate. In [86], a simulation study and extension of the single-cell thermal model were utilized to examine the thermal modeling of LIB. The single-cell model has been reported to prove remarkably accurate. However, some assumptions have been made to extend it to battery cells, including 100% efficient discharge processes, constant environmental conditions, and uniform cell properties, which do not correspond to real-life conditions, and the scenes are very different. Therefore, additional research into the accuracy of the temperature estimating approach in real-world settings is required. As a result, as was clear from prior discussion, package-level labeling schemes merit more research. For easy reader reference, Table 2 lists the EECM-based temperature estimating techniques put out by various writers. The requirement for online feedback from the sensor is one of the critical drawbacks of EECM-based temperature estimating techniques. Due to battery aging, operation, temperature, and other practical uncertainties, the accuracy of the assessment solely depends on the accuracy of the informa-

tion provided on the thermal characteristics of the battery, the rate of heat release, and the limits of thermal conditions given in the form of electrical parameters.

Table 2

An overview of temperature estimating techniques based on EECM

#	Model
[70]	LP heat capacitance-resistance thermal model
[43]	LP, single-state, FOM
[13]	LP, TSM, SOM + Kalman filter (KF)
[74]	LP, TSM, SOM
[75]	Extended LP, TS, SOM + forgetting factor recursive least squares (FFRLS)
[45] and [76]	LP, two-state model (TSM) + least squares (LS) algorithm + nonuniform forgetting factors (NUFF)
[77]	LP model + closed-loop observer
[78]	LP, SOM, single-state thermal model + KF
[79]	LP, SOM, TSM + JFK + LS algorithm
[80] and [71]	LP, TSM + extended KF
[72]	LP, TSM + joint KF (JKF)
[19]	LP, second-order, multi-node model + particle-swarm algorithm
[81]	1D (radial) LP, three node model + dual KF (DKF).
[82]	LP, single-state model + extended unscented KF (EUKF)
[83]	LP, TSM + extended state observer (ESO)
[14]	LP, single-state thermal model + KF + recursive least squares (RLS) algorithm
[84]	EECM-based virtual thermal sensors (VTS) + KF
[85] and [86]	ROM of a LIB pack for a central temperature of LIB pack + recursive least squares (RLS)

4.3. Numerical analysis-based TES

The temperature of LIB cells and even LIB batteries with various chemical compositions and forms have been accurately estimated using numerical approaches. For estimating temperature thus far, the finite element method (FEM) [87–90] and the finite volume approach (FVM) [91] have been extensively employed. Methods based on numerical analysis try to use nonlinear partial differential equations (PDEs), such as those developed by [89], to mathematically explain the thermodynamics of a battery. Based on Bernard's equation and the rate of internal heating, a 3D model was employed in conjunction with FEM analysis. The boundary conditions for PDEs are frequently intricate and have infinite dimensions. The fundamental mathematical formula equation can be used to express (5) [89]:

$$\rho C_p \frac{\partial T}{\partial t} = \lambda_x \frac{\partial^2 T}{\partial x^2} + \lambda_y \frac{\partial^2 T}{\partial y^2} + \lambda_z \frac{\partial^2 T}{\partial z^2} + Q. \quad (5)$$

The average density and specific heat of the battery are used, respectively, with C_p among them. The battery's surface material's thermal conductivity, and Q is the same as in formula (1).

To comprehend the thermal performance of commercial LIBs under charge and discharge conditions, [87] integrated a transient thermoelectric model (TTM) with a porous electrode model and conducted numerical simulations. He proved that temperature increase occurs more rapidly during discharge than during charging. He added that raising the C rate might help to lessen the temperature differential between charging and discharging. A better single-event LIB model was numerically simulated by [88] to comprehend the 3D temperature distribution in the battery. The transient behavior of LIBs during dynamic conduction cycles was numerically analyzed by [90]. Double-layer thermal capacitors are used to rectify short-term transient voltages in LIB chemical composition. In their study utilizing FVM, [91] demonstrated how temperature gradients in battery layers result in various current densities and local SOC imbalances in LIBs. These phenomena must be considered thoroughly when creating an effective thermal management system. Since a battery's thermal process is a typical system of distributed characteristics, this model is generally best suited for describing a battery's temporal and spatial thermal behavior. Despite their incredible accuracy and in-depth understanding of battery temperatures, these numerical temperature estimation approaches are not appropriate for online temperature estimation due to their high computing costs. Complex mathematical analysis calls for both specialized expertise and in-depth subject understanding. Furthermore, due to variations in cell chemistry and physics that have an impact on mathematical modeling, generality is not attainable. The numerical approach for estimating temperature is summarized in Table 3.

Table 3

Summary of numerical method-based TES

Model	Synopsis
A TTM with a porous electrode model + finite element method (FEM) [87]	various driving scenarios, simulation using COMSOL Multiphysics (COMSOL Inc., Stockholm, Sweden), and experimental verification
Enhanced single-particle model + FEM [88]	Validation of the 3D temperature distribution within the cell, as well as cell geometry and current profile, through experimentation
3D model + ECM-based HGM + FEM [89]	Variable temperature, various current profiles, COMSOL Multiphysics modeling, and experimental validation
TTM + FEM [90]	momentary actions during a dynamic driving cycle validated through experiment
3D model + FVM [91]	Simulations in MATLAB and experimental confirmation of inhomogeneities in non-current density and local SOC over many cell layers.

4.4. Direct impedance measurement-based temperature estimation

There are several issues with estimating internal battery temperature using local and coarse-grained thermal models. First, it is challenging to calculate the model's thermal qualities, such as its thermal conductivity and the battery's thermal conductivity. The operating current, voltage and internal resistance of the battery – which are also functions of SOC, internal battery temperature and SOH – are typically used to determine the amount of heat produced in batteries. Furthermore, the thermal contact resistance between layers of a battery made of various materials that have been integrated into a layered structure is frequently unknown. Surface temperature measurements are used in TES. Even a combination of surface temperature sensors and thermal models frequently fails to detect the temperature because rapid changes in internal temperature are difficult to capture with surface sensors because of inter-core heat conduction. This is time-consuming [92]. Regarding manufacturing complexity and system cost, it is nearly impossible to include a small temperature sensor in a battery [93,94] for high-capacity LIB batteries. Therefore, using physical sensors to measure room temperature is inappropriate for industrial applications. The phase of electrochemical resistance in the frequency range of 40 to 100 Hz is sensitive to temperature, but not to changes in other parameters such as SOC and SOH, according to [95,96]. Based on these findings, they present an electrochemical barrier-based technique to gauge the interior temperature of batteries. However, the categorization approach is only applicable in the temperature range of -20 to 66°C , and they assume that the internal temperature is constant as proved by [97]. Investigated temperature calculations that consider non-uniform temperature effects on electrochemical resistance are based on the guidelines provided by [98]. However, in real-world applications, especially for cylindrical batteries with high charge and discharge currents, the difference between the maximum internal temperature, surface temperature and average temperature is very significant. We can only estimate the average cell temperature. To precisely establish the internal temperature distribution, [3] expanded the investigation. They created a thermal resistance model by fusing single frequency EIS data with surface temperature measurements. Figure 4 illustrates a fundamental procedure for temperature estimation based on direct resistivity measurements performed by [3]. According to [3], the critical constraint is determining each battery's linear resistance, which is highly challenging. It is optional to know the thermal parameters of the battery, thermal conductivity, or thermal conditions. Additionally, each cell would need a surface temperature sensor, which is currently impractical without environmental variability. Additionally, looking at the systematic analysis of resistance measurements when direct current is present proves essential. Although several techniques for employing onboard electronics in EVs to determine impedance spectra online at various frequencies have been disclosed [99], the use of these techniques to estimate temperature in real time has yet to be studied.

Impedance temperature detection (ITD), a sensor less online TES based on EIS that considers battery age and uncertainty, was proposed by [100]. This approach combines surface mount

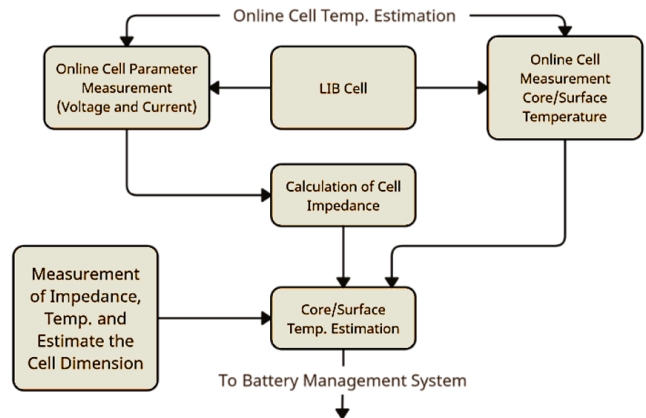


Fig. 4. Basic procedures for determining temperature using direct impedance measurements

sensors with ITD to precisely estimate network temperature because TGD alone cannot offer a complete answer [3]. However, it is necessary to attach a temperature sensor. Based on this research, they combined ITD with an electrothermal model and DEKF to estimate a LIB battery's core temperature online, even without a known heating factor. Additionally, they demonstrated that the TGD with surface temperature sensors functioned virtually and presented the ITD thermal model. Despite these benefits, the principal downsides of this approach are the requirement for precise electrothermal modeling and online resistance calculation, which share the same shortcomings as conventional thermal modeling techniques. Furthermore, this work needs to show a way for batch-level estimation, even though this method can estimate individual cells' basal and surface temperatures.

The impact of battery temperature, SOC and SOH on the impedance spectra, transmission frequency and precision of internal battery temperature estimation was studied by [101]. Here, a matrix analysis of the impedance response created by EIS measurements is used to estimate the temperature. Although precise, it needs to account for the impact of varying battery temperatures and maintenance techniques. It is challenging to identify the proper frequency and other EIS parameters, and the accuracy of the estimation is heavily dependent on these factors. Additionally, extensive experimental research and significant computational resources are needed for the simulation. As a result, it is challenging to apply this method online.

Additionally, it is exceedingly challenging to distinguish between the real and imaginary components of resistance. Using a different definition for the two components can result in estimations of temperature that prove off. To determine the battery temperature, [102] proposed combining a multi-objective observer-based method and a thermal acceleration model (LPV). [3, 103–106] have also utilized EIS-based techniques to estimate interior temperatures. Despite excellent accuracy, the key restriction is the need for time-consuming preliminary experiments to determine the precise temperature and resistance characteristics. Additionally, their heat resistance changes when batteries age, causing SOH degradation and erroneous projections. The TES based on direct resistance measurement is summarized in Table 4.

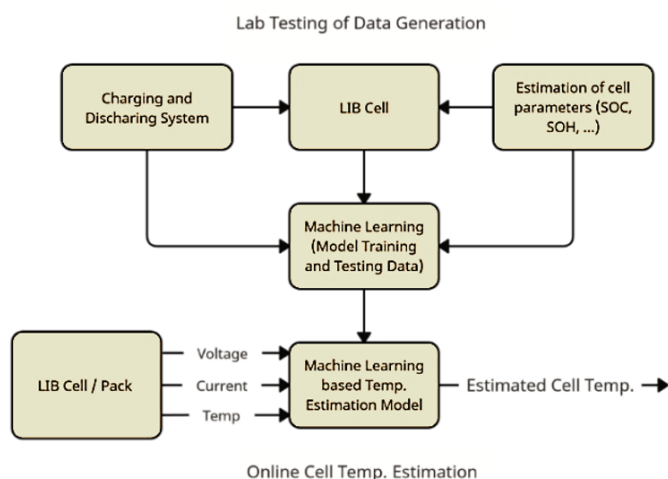
Table 4

Summary of direct impedance measurement-based strategies

Model	Synopsis
Direct electrochemical impedance measuring [95, 96]	Experimental verification using information from EIS
Direct electrochemical impedance measuring [97]	Temperature fluctuation was not considered; experimentally confirmed
Thermal-impedance model + EIS measurement at single frequency + surface temperature feedback [3]	Experimental validation utilizing EIS data can be performed regardless of the thermal characteristics of the cell, the amount of heat generated, or the thermal boundary conditions
Online EIS measurement (impedance-temperature detection (ITD) + dual-extended Kalman filter (DEKF) [100]	Considering a convection coefficient that is unknown to us, this theory has been verified empirically
Measurements from an EIS were used to generate an analysis of the impedance response matrix [101]	Impedance spectroscopy: temperature, state-of-charge, and state-of-health-cell influences, experimental confirmation using EIS data

4.5. ML-based TES

The thermodynamic behavior of a battery varies significantly from its core to its surface due to its exceedingly intricate electrochemical reactions and its sensitivity to environmental uncertainty. The spatial and temporal distribution of LIBs, particularly large-capacity batteries, cannot be accounted for by most distributed thermal models and spatial thermal models now in use. Additionally, depicting these space-time interactions with a single physical model is challenging. Here, local dynamics are frequently preserved using ML approaches to increase the modeling precision of nonlinear systems such as LIBs. Figure 5

**Fig. 5.** Schematic layout of ML-based TES

displays a schematic representation of a temperature estimation system based on ML.

[107] created a local thermodynamic LIB model to precisely estimate the interior temperature distribution using a hybrid EECM model and neural network (NN)-based learning techniques. The data driven NN model employs standard BMS metrics to correct trade model inconsistencies brought on by spatial nonlinearity and other model errors. [109] examined LIB based on NN [108] and the support vector machine (SVM). To determine the internal temperature of LIBs, [110] introduced a hybrid radial basis function neural network (RBFNN) and EKF model. These models' primary objective is to predict SOC or SOH, not to estimate battery temperature, even if they consider how temperature affects battery performance. Generalization is one of the critical issues with systems that only use ML. By merging electrochemical thermal, feed-forward neural network (FFNN) and UKF, [111] created an effective electrochemical-thermal-neural network (ETNN). The technique performs admirably in SOT prediction over a broad temperature range and in high-current environments. The simulation is intricate and has yet to be tested to see how accurate different charging currents and driving cycles are.

Additionally, web applications' efficacy and usability are in doubt. The electrochemical model on ETNN's reverse has the same drawbacks as the electrochemical model. ML-based diagrams are generally computationally efficient, but gathering data and building a model is difficult and time-consuming. Additionally, accurate battery test data still need to be addressed in the available literature when training ML-based models; as a result, the accuracy of current ML-based solutions is still debatable. The approaches based on ML presented by researchers are compiled in Table 5.

Table 5

Summary of ML-based TES

Model Type	Synopsis
EECM + neural network (NN)-based learning approach [107]	Inaccurate representation of the plant in the model due to spatial nonlinearity and other modeling problems; the NN-model was verified by experimental data
NN + support vector machines [109]	Using real-world data, the effects of environmental factors such as temperature, charging current, Python (Python Software Foundation, Wilmington, DE, USA), neural networks, and support machines (SVMs) were examined
RBF neural network (RBNN) and the extended Kalman filter (EKF) [110]	The effect that temperature has on the behavior of cells, as proven by simulation data
Electrochemical-thermal-neural network (ETNN) + unscented Kalman filter (UKF) [111]	Python settings covering a wide temperature range and a considerable amount of current, proven using data from experiments

4.6. Magnetic nanoparticles-based TES

The relationship between the third and fifth harmonic responses can be used to measure the internal temperature of magnetic nanoparticles (MNPs), whose magnetization is nonlinear in an alternating magnetic field [112, 113]. Additionally, [114] investigated the thermal sensitivity of MNPs to an increase in a constant magnetic field. It was discovered that as the constant magnetic field increased, the thermal sensitivity of MNPs decreased. Based on the findings of this study, [115] created an advanced magnetic nanoparticle thermometer (MNPT) that uses magnetic nanoparticle thermometry to determine the LIB core temperature (MNP). They also recommended a range of DC magnetic field strengths to provide the highest possible temperature sensitivity and the lowest possible MNPT temperature inaccuracy. Please note that this type of evaluation topology is quite costly and massive. Additionally, the utility of online forecasts has yet to be assessed.

5. DISCUSSION

Depending on the amount of accuracy required and the accuracy of the prediction findings, the LIB temperature estimate system can be put together in various ways. Comprehensive simulation results and the most precise projections are required for the BMS to operate safely and dependably. However, adding more specific battery phenomena to the model eventually makes it more complex, costs more money to run, and limits site forecasts and BMS use for low-cost flights. For instance, the computation model becomes more complicated if the temperature of each cell layer is considered rather than the core's high heating. Secondly, rather than just radial for simplicity, heat movement into and

out of the battery can be thought of in both axial and radial directions.

Furthermore, while simpler models consider conductive heat transfer, complex models typically consider several mechanisms of heat transmission, including conduction, convection and radiation. Significant parameters are needed to include more phenomena in a thermal simulation, which increases the need for experimental data, simulation time and solid-area knowledge. A detailed and thorough understanding of battery design, material qualities and composition is also necessary. However, because the design data are proprietary, getting this information from battery makers is challenging. From the preceding explanation, while intricate models can give an exact and thorough representation of battery thermodynamics, their computational complexity may render them unsuitable for real-time and airborne BMS prediction. In general, physical sensor readings are needed for most evaluation methods. However, large LIBs with thousands of individual cells make it practically impossible to place a physical sensor in every cell.

Additionally, embedding a sensor to gauge the temperature of the battery core is quite challenging. Various rating systems use surface temperature sensors to infer inside temperatures. This is entirely incorrect, though, as heat moves slowly from the core to the surface. Most research to date has concentrated on Li-ion battery temperature rating techniques. Calculating the temperature of LIB batteries is more challenging. Therefore, extensive additional research is advised in this area. In-depth research is yet to be done on how quick charge/discharge affects battery temperature – highly advised for the growth of BMS with a focus on health. The issues, difficulties and recommendations of potential study areas for the research community are summarized in Table 6.

Table 6

Summary of major issues, challenges and research recommendations

Strategy	Major issues and challenges	Recommendations
Electrochemical model-based	<ul style="list-style-type: none"> • Very accurate modeling is possible. Therefore, it can provide very accurate predictions but at a very high computational cost. Therefore, it is not suitable for online BMS prediction. • In addition to mathematical modeling expertise, detailed knowledge of LIB chemistry is required, allowing one to rely on industry experts. • Extensive testing is required to gather detailed information on battery properties. • Modeling is complicated. • Designing adaptive signaling systems is exceptionally complex. • Low ability to generalize. 	<ul style="list-style-type: none"> • Offers meaningful future research opportunities to reduce modeling complexity and computational cost. • Provides best predictive results to date, so it can be widely used to test other models and provide data for data-driven models. • LIB chemistry is susceptible to temperature, battery conditions, and other uncertainties. Therefore, further study of adaptive models is recommended.
EECM model-based	<ul style="list-style-type: none"> • Most often used today, high accuracy, easy to use, but with an increase in the order of the models, the number of points (nodes) of temperature measurements and the distribution of parameters, the complexity of modeling, and the increase in the cost of calculations. • Accurate EECM parameters are difficult to determine, especially online parameter estimation. 	<ul style="list-style-type: none"> • Trade-offs between accuracy requirements and model detail can control simulation complexity and computational cost. • Adaptive skills are complex, but by incorporating advanced algorithms (e.g. ML-based methods), adaptive strategies can be developed.

Table 6 [cont.]

Strategy	Major issues and challenges	Recommendations
EECM model-based	<ul style="list-style-type: none"> Parameter setting with external measurements is complex and time-consuming. Very few researchers also use electrochemical analysis to detect and define variables, which presents the same difficulties as electrochemical methods. Prediction is heavily affected by measurement noise and often requires too many physical sensors. Until now, smaller/minimum models have been widely used for online forecasting due to their accuracy and detailed analysis. 	<ul style="list-style-type: none"> These models can provide very accurate results in the laboratory and can therefore be used to generate data and validate models for other methods. Combining this strategy with other methods, such as ML methods, can improve accuracy and computational performance. Instead of traditional filters, advanced adaptive filtering techniques can be used to improve performance.
ML-based	<ul style="list-style-type: none"> Data-driven black box policy, i.e. the predictions are based solely on external measurements, so little or no domain knowledge is required. However, the main challenge is to collect quality data for in-depth training. No complex iterative mathematical calculations are required, so the computational cost is sufficient for online applications. However, the computational cost increases for more information with more extensive data (high resolution) and many feature vectors. High-resolution data collection, primarily manufacturer and error data, is complicated. This data is essential for accurate and adaptive forecasting. Generalization is difficult. Not currently used in automotive BMS due to long learning times, complex algorithm development, and computation time, given that little has been done so far. External measurement of physical sensors is usually required as feedback for online parameter setting, so it is still necessary to install physical sensors. 	<ul style="list-style-type: none"> Although it is relatively easy to develop adaptive models, more effort is required. Battery properties are greatly affected by uncertain factors such as temperature and aging, so further investigation of adaptive modeling is recommended. Generalization is difficult but possible with sophisticated adaptive algorithms. With proper design, it can be used for web forecasting and implemented in BMS with low processing power. Very promising methodology for next-generation sensor-less TES. So far, little has been attempted; therefore, further research is recommended.
Numerical model-based	<ul style="list-style-type: none"> These methods use FEA and FVA. The TES based on FEA and FVA was the most accurate and computationally expensive. Its computational cost is high due to complex and repetitive mathematical calculations, so it is unsuitable for online prediction. 	<ul style="list-style-type: none"> Significant research and development work is needed to reduce computational cost and adapt it to online predictions. Because it is the most accurate, it can validate the model further and collect accurate data.
Direct impedance measurement-based	<ul style="list-style-type: none"> The effect of temperature on battery resistance is used to estimate internal temperature. However, it is challenging to measure resistance directly online using integrated electronics. Since the change in battery resistance due to temperature changes is small, it is difficult to determine this small change accurately. The current program is pervasive. Little research has been done to date, and no real action has yet been taken. 	<ul style="list-style-type: none"> Therefore, promising technologies and significant additional research and development are recommended to reduce the program's scope and evaluate the practical utility of airborne BMS. The need to assess accuracy in practical use Further research into using embedded electronics to determine line resistance is also recommended. The cost of current solutions is very high and must be considered.
Magnetic nanoparticle-based	<ul style="list-style-type: none"> Very recent technology; too soon to make any judgments. 	<ul style="list-style-type: none"> Onboard low-cost BMS's practical usefulness is yet to be researched. Overall, extensive additional research is needed.

6. CONCLUSIONS

The most recent thermal testing techniques for LIBs are covered in detail in this article, along with the need for the best test procedures, the methods that are already in use, any issues they may present, and suggestions. Accurate LIB temperature estimation is crucial for BMSs' effective thermal management, operational safety and various other activities (BMS). Physical

sensors are nearly useless for determining each cell's temperature, particularly in large-capacity batteries that include hundreds of different cells. It is essential to concentrate on some aspects while creating an ideal temperature estimate circuit, including high precision, high adaptability, small size, real-time estimation, distribution (battery assembly temperature monitoring), low cost, and simplicity of use. A temperature estimation system typically consists of two models: one for heat release and

the other for heat transfer. Temperature estimation circuits are classified into six types based on their modeling and calculation techniques: electrochemical computational modeling, EECM, ML, digital analysis and direct impedance measurement. Magnetic nanoparticles serve as a basis. The most precise methods are based on numerical analysis, followed by electrochemical models. Unfortunately, because of the high computational costs of both methods, none of them can forecast the low-cost integrated BMS in real time.

Additionally, there are very high needs for complicated simulation and experimentation, as well as a need for subject expertise. Different levels of EECM-based circuit complexity, precision and computational expense are possible. In both literature and practice, minimal simplified EECM diagrams are frequently utilized. Diagrams created using ML have the potential to be very accurate, simple to use and adaptable. However, obtaining feature vectors necessitates a substantial amount of high-quality data, which is frequently challenging. A hybrid approach fusing EECM with ML might be an appropriate resolution in this situation. Direct resistivity measurements and magnetic nanoparticle-based techniques have recently been established. It is still too early to judge their suitability for online prediction and implementation in automotive BMS and their capabilities. As a result, the systematic alignment of active research fields and potential future research directions are emphasized in this work. Additionally, it should be emphasized that while most papers include TES for individual LIB cells, temperature estimation for LIB batteries is more complicated.

REFERENCES

- [1] X. Zhang, Z. Li, L. Luo, Y. Fan, and Z. Du, "A review on thermal management of lithium-ion batteries for electric vehicles," *Energy*, vol. 238, p. 121652, 2022, doi: [10.1016/j.energy.2021.121652](https://doi.org/10.1016/j.energy.2021.121652).
- [2] G. Karimi and X. Li, "Thermal management of lithium-ion batteries for electric vehicles," *Int. J. Energy Res.*, vol. 37, pp. 13–24, 2013. doi: [10.1002/er.1956](https://doi.org/10.1002/er.1956).
- [3] R.R. Richardson, P.T. Ireland, and D.A. Howey, "Battery internal temperature estimation by combined impedance and surface temperature measurement," *J. Power Sources*, vol. 265, pp. 254–261, 2014, doi: [10.1016/j.jpowsour.2014.04.129](https://doi.org/10.1016/j.jpowsour.2014.04.129).
- [4] G. Liu *et al.*, "Analysis of the heat generation of lithium-ion battery during charging and discharging considering different influencing factors," *J. Therm. Anal. Calorim.*, vol. 116, pp. 1001–1010, 2014, doi: [10.1007/s10973-013-3599-9](https://doi.org/10.1007/s10973-013-3599-9).
- [5] X. Lin, Y. Kim, S. Mohan, J.B. Siegel, and A.G. Stefanopoulou, "Modeling and Estimation for Advanced Battery Management," *Annu. Rev. Contr. Robot. Autonom. Syst.*, vol. 2, pp. 393–426, 2019. doi: [10.1146/annurev-control-053018-023643](https://doi.org/10.1146/annurev-control-053018-023643).
- [6] S. Pang, J. Farrell, J. Du, and M. Barth, "Battery state-of-charge estimation," *Proc. 2001 American Control Conference, USA*, 2001, vol. 2, pp. 1644–1649, doi: [10.1109/ACC.2001.945964](https://doi.org/10.1109/ACC.2001.945964).
- [7] H. Sun, D. Yang, L. Wang, and K. Wang, "A method for estimating the aging state of lithium-ion batteries based on a multi-linear integrated model," *Int. J. Energy Res.*, vol. 46, pp. 24091–24104, 2022. doi: [10.1002/er.8709](https://doi.org/10.1002/er.8709).
- [8] M. Zhang *et al.*, "A Review of SOH Prediction of Li-Ion Batteries Based on Data-Driven Algorithms," *Energies*, vol. 16, p. 3167, 2023, doi: [10.3390/en16073167](https://doi.org/10.3390/en16073167).
- [9] Z. Zhang, L. Zhang, L. Hu, and C. Huang, "Active cell balancing of lithium-ion battery pack based on average state of charge," *Int. J. Energy Res.*, vol. 44, pp. 2535–2548, 2020, doi: [10.1002/er.4876](https://doi.org/10.1002/er.4876).
- [10] W. Zhang, X. Li, and X. Li, "Deep learning-based prognostic approach for lithium-ion batteries with adaptive time-series prediction and on-line validation," *Measurement*, vol. 164, p. 108052, 2020, doi: [10.1016/j.measurement.2020.108052](https://doi.org/10.1016/j.measurement.2020.108052).
- [11] A. Senyshyn, M.J. Mühlbauer, O. Dolotko, and H. Ehrenberg, "Low-temperature performance of Li-ion batteries: The behavior of lithiated graphite," *J. Power Sources*, vol. 282, pp. 235–240, 2015, doi: [10.1016/j.jpowsour.2015.02.008](https://doi.org/10.1016/j.jpowsour.2015.02.008).
- [12] J. Jagemont, L. Boulon, P. Venet, Y. Dubé, and A. Sari, "Lithium-Ion Battery Aging Experiments at Subzero Temperatures and Model Development for Capacity Fade Estimation," *IEEE Trans. Veh. Technol.*, vol. 65, no. 6, pp. 4328–4343, June 2016, doi: [10.1109/TVT.2015.2473841](https://doi.org/10.1109/TVT.2015.2473841).
- [13] S. Surya, V. Marcis, and S. Williamson, "Core Temperature Estimation for a Lithium-ion 18650 Cell," *Energies*, vol. 14, 87, 2020. doi: [10.3390/en14010087](https://doi.org/10.3390/en14010087).
- [14] S. Surya, and Ajrun MN, "Effect of Fast Discharge of a Battery on its Core Temperature," *2020 International Conference on Futuristic Technologies in Control Systems & Renewable Energy (ICFCR)*, 2020, pp. 1–6, doi: [10.1109/ICFCR50903.2020.9249999](https://doi.org/10.1109/ICFCR50903.2020.9249999).
- [15] Z. Wei, J. Zhao, H. He, G. Ding, H. Cui, and L. Liu, "Future smart battery and management: Advanced sensing from external to embedded multi-dimensional measurement," *J. Power Sources*, vol. 489, p. 229462, 2021, doi: [10.1016/j.jpowsour.2021.229462](https://doi.org/10.1016/j.jpowsour.2021.229462).
- [16] S. Orcioni, L. Buccolini, A. Ricci, and M. Conti, "Lithium-ion Battery Electrothermal Model, Parameter Estimation, and Simulation Environment," *Energies*, vol. 10, p. 375, 2017, doi: [10.3390/en10030375](https://doi.org/10.3390/en10030375).
- [17] M. Rouholamini *et al.*, "A Review of Modeling, Management, and Applications of Grid-Connected Li-Ion Battery Storage Systems," *IEEE Trans. Smart Grid*, vol. 13, pp. 4505–4524, 2022, doi: [10.1109/TSG.2022.3188598](https://doi.org/10.1109/TSG.2022.3188598).
- [18] J. Fleming, T. Amietszajew, J. Charmet, A.J. Roberts, D. Greenwood, and R. Bhagat, "The design and impact of in-situ and operando thermal sensing for smart energy storage," *J. Energy Storage*, vol. 22, pp. 36–43, 2019, doi: [10.1016/j.est.2019.01.026](https://doi.org/10.1016/j.est.2019.01.026).
- [19] Y. Ye, Y. Shi, N. Cai, J. Lee, and X. He, "Electro-thermal modeling and experimental validation for lithium-ion battery," *J. Power Sources*, vol. 199, pp. 227–238, 2012. doi: [10.1016/j.jpowsour.2011.10.027](https://doi.org/10.1016/j.jpowsour.2011.10.027).
- [20] H. He and X. Chen, "Analysing unbalanced ageing in EV battery Packs using the Low-Cost Lumped Single Particle Model (LSPM): the impact of temperature gradients among parallel-connected cells," *Transp. Res. Procedia*, vol. 70, pp. 406–413, 2019, doi: [10.1016/j.trpro.2023.11.046](https://doi.org/10.1016/j.trpro.2023.11.046).
- [21] A.A. El Baset A. El Halim, E.H. Eid Bayoumi, W. El-Khattam, and A.M. Ibrahim, "Development of robust and accurate thermo-electrochemical models for Lithium-ion batteries", *e-Prime-Adv. Electr. Eng. Electron. Energy*, vol. 6, p. 100342, 2023, doi: [10.1016/j.prime.2023.100342](https://doi.org/10.1016/j.prime.2023.100342).

- [22] B. Sun, X. Qi, D. Song, and H. Ruan, "Review of Low-Temperature Performance, Modeling and Heating for Lithium-Ion Batteries," *Energies*, vol. 16, p. 7142, 2023, doi: [10.3390/en16207142](https://doi.org/10.3390/en16207142).
- [23] C. Zhu, X. Li, L. Song, and L. Xiang, "Development of a theoretically based thermal model for lithium ion battery pack", *J. Power Sources*, vol. 223, pp. 155–164, 2013, doi: [10.1016/j.jpowsour.2012.09.035](https://doi.org/10.1016/j.jpowsour.2012.09.035).
- [24] R. Klein, N.A. Chaturvedi, J. Christensen, J. Ahmed, R. Findenisen and A. Kojic, "Electrochemical Model Based Observer Design for a Lithium-Ion Battery," *IEEE Trans. Control Syst. Technol.*, vol. 21, pp. 289–3, 2013, doi: [10.1109/TCST.2011.2178604](https://doi.org/10.1109/TCST.2011.2178604).
- [25] Y. Chen *et al.*, "A review of lithium-ion battery safety concerns: The issues, strategies, and testing standards," *J. Energy Chem.*, vol. 59, pp. 83–99, 2021, doi: [10.1016/j.jechem.2020.10.017](https://doi.org/10.1016/j.jechem.2020.10.017).
- [26] X.-G. Yang, Y. Leng, G. Zhang, S. Ge, and C.-Y. Wang, "Modeling of lithium plating induced aging of lithium-ion batteries: Transition from linear to nonlinear aging," *J. Power Sources*, vol. 360, pp. 28–40, 2017, doi: [10.1016/j.jpowsour.2017.05.110](https://doi.org/10.1016/j.jpowsour.2017.05.110).
- [27] L. Song and J.W. Evans, "Electrochemical-Thermal Model of Lithium Polymer Batteries," *J. Electrochem. Soc.*, vol. 147, p. 2086, 2000, doi: [10.1149/1.1393490](https://doi.org/10.1149/1.1393490).
- [28] W. Allafi *et al.*, "A lumped thermal model of lithium-ion battery cells considering radiative heat transfer," *Appl. Therm. Eng.*, vol. 143, pp. 472–481, 2018, doi: [10.1016/j.applthermaleng.2018.07.105](https://doi.org/10.1016/j.applthermaleng.2018.07.105).
- [29] S. Tamilselvi *et al.*, "A Review on Battery Modelling Techniques," *Sustainability*, vol. 13, p. 10042, 2021, doi: [10.3390/su131810042](https://doi.org/10.3390/su131810042).
- [30] C. Zhang, K. Li, S. Mcloone, and Z. Yang, "Battery modeling methods for electric vehicles – A review," *2014 European Control Conference (ECC)*, 2014, doi: [10.1109/ECC.2014.6862541](https://doi.org/10.1109/ECC.2014.6862541).
- [31] H. Hinz, "Comparison of Lithium-Ion Battery Models for Simulating Storage Systems in Distributed Power Generation," *Inventions*, vol. 4, p. 41, 2019, doi: [10.3390/inventions4030041](https://doi.org/10.3390/inventions4030041).
- [32] M. Gilaki and I. Avdeev, "Impact modeling of cylindrical lithium-ion battery cells: a heterogeneous approach," *J. Power Sources*, vol. 328, pp. 443–451, 2016, doi: [10.1016/j.jpowsour.2016.08.034](https://doi.org/10.1016/j.jpowsour.2016.08.034).
- [33] M. Safari and C. Delacourt, "Mathematical Modeling of Lithium Iron Phosphate Electrode: Galvanostatic Charge/Discharge and Path Dependence," *J. Electrochem. Soc.*, vol. 158, p. A63, 2011, doi: [10.1149/1.3515902](https://doi.org/10.1149/1.3515902).
- [34] Y. Xiao and B. Fahimi, "State-space based multi-nodes thermal model for lithium-ion battery," *Proc. IEEE Transportation Electrification Conference and Expo: Components, Systems, and Power Electronics – From Technology to Business and Public Policy, ITEC 2014*, 2014, doi: [10.1109/ITEC.2014.6861846](https://doi.org/10.1109/ITEC.2014.6861846).
- [35] Y.-W. Pan *et al.*, "A computational multi-node electro-thermal model for large prismatic lithium-ion batteries," *J. Power Sources*, vol. 459, p. 228070, 2020, doi: [10.1016/j.jpowsour.2020.228070](https://doi.org/10.1016/j.jpowsour.2020.228070).
- [36] N. Tian, H. Fang, and Y. Wang, "3-D Temperature Field Reconstruction for a Lithium-Ion Battery Pack: A Distributed Kalman Filtering Approach," *IEEE Trans. Control Syst. Technol.*, vol. 27, pp. 847–854, 2019, doi: [10.48550/arXiv.1709.08819](https://doi.org/10.48550/arXiv.1709.08819).
- [37] B. Mao, C. Zhao, H. Chen, Q. Wang, and J. Sun, "Experimental and modeling analysis of jet flow and fire dynamics of 18650-type lithium-ion battery", *Appl. Energy*, vol. 281, p. 116054, 2021, doi: [10.1016/j.apenergy.2020.116054](https://doi.org/10.1016/j.apenergy.2020.116054).
- [38] H. Ruan, J. Jiang, B. Sun, W. Gao, L. Wang, and W. Zhang, "On-line estimation of thermal parameters based on a reduced wide-temperature-range electro-thermal coupled model for lithium-ion batteries," *J. Power Sources*, vol. 396, pp. 715–724, 2018, doi: [10.1016/j.jpowsour.2018.03.075](https://doi.org/10.1016/j.jpowsour.2018.03.075).
- [39] T. Wang, K.J. Tseng, J. Zhao, and Z. Wei, "Thermal investigation of lithium-ion battery module with different cell arrangement structures and forced air-cooling strategies," *Appl. Energy*, vol. 134, pp. 229–238, 2014, doi: [10.1016/j.apenergy.2014.08.013](https://doi.org/10.1016/j.apenergy.2014.08.013).
- [40] B. Liu, S. Yin, and J. Xu, "Integrated computation model of lithium-ion battery subject to nail penetration," *Appl. Energy*, vol. 183, pp. 278–289, 2016, doi: [10.1016/j.apenergy.2016.08.101](https://doi.org/10.1016/j.apenergy.2016.08.101).
- [41] S. Anwar, C. Zou, and C. Manzie, "Distributed Thermal-Electrochemical Modeling of a Lithium-Ion Battery to Study the Effect of High Charging Rates", *IFAC Proc. Vol.*, vol. 47, pp. 6258–6263, 2014, doi: [10.3182/20140824-6-ZA-1003.00919](https://doi.org/10.3182/20140824-6-ZA-1003.00919).
- [42] K. Kumaresan, G. Sikha, and R.E. White, "Thermal Model for a Li-Ion Cell," *J. Electrochem. Soc.*, vol. 155, p. A164, 2008, doi: [10.1149/1.2817888](https://doi.org/10.1149/1.2817888).
- [43] C. Forgez, V.D. Do, G. Friedrich, M. Morcrette, and C. Delacourt, "Thermal modeling of a cylindrical LiFePO₄/graphite lithium-ion battery," *J. Power Sources*, vol. 195, pp. 2961–2968, 2010, doi: [10.1016/j.jpowsour.2009.10.105](https://doi.org/10.1016/j.jpowsour.2009.10.105).
- [44] D.W. Dees, V.S. Battaglia, and A. Bélanger, "Electrochemical modeling of lithium polymer batteries," *J. Power Sources*, vol. 110, pp. 310–320, 2002, doi: [10.1016/S0378-7753\(02\)00193-3](https://doi.org/10.1016/S0378-7753(02)00193-3).
- [45] S. Ludwig, M. Steinhardt, and A. Jossen, "Determination of Internal Temperature Differences for Various Cylindrical Lithium-Ion Batteries Using a Pulse Resistance Approach," *Batteries*, vol. 8, p. 60, 2022, doi: [10.3390/batteries8070060](https://doi.org/10.3390/batteries8070060).
- [46] M. Walter, M.V. Kovalenko, and K.V. Kravchyk, "Challenges and benefits of post-lithium-ion batteries," *New J. Chem.*, vol.44, no. 5, pp. 1677–1683, 2020, doi: [10.1039/C9NJ05682C](https://doi.org/10.1039/C9NJ05682C).
- [47] M. Petzl, M. Kasper, and M.A. Danzer, "Lithium plating in a commercial lithium-ion battery – A low-temperature aging study," *J. Power Sources*, vol. 275, pp. 799–807, 2015, doi: [10.1016/j.jpowsour.2014.11.065](https://doi.org/10.1016/j.jpowsour.2014.11.065).
- [48] P. Ping, Q. Wang, Y. Chung, and J. Wen, "Modeling electro-thermal response of lithium-ion batteries from normal to abuse conditions," *Appl. Energy*, vol. 205, pp. 1327–1344, 2017, doi: [10.1016/j.apenergy.2017.08.073](https://doi.org/10.1016/j.apenergy.2017.08.073).
- [49] Al-S. Hallaj and J.R. Selman, "Thermal modeling of secondary lithium batteries for electric vehicle/hybrid electric vehicle applications," *J. Power Sources*, vol. 110, no. 2, pp. 341–348, 2002, doi: [10.1016/S0378-7753\(02\)00196-9](https://doi.org/10.1016/S0378-7753(02)00196-9).
- [50] T.F. Fuller, M. Doyle, and J. Newman, "Simulation and Optimization of the Dual Lithium-Ion Insertion Cell," *J. Electrochem. Soc.*, vol. 141, pp. 1–10, 1994, doi: [10.1149/1.2054684](https://doi.org/10.1149/1.2054684).
- [51] S.S. Madani, E. Schaltz, and S.K. Kær, "Review of Parameter Determination for Thermal Modeling of Lithium Ion Batteries," *Batteries*, vol. 4, p. 20, 2018, doi: [10.3390/batteries4020020](https://doi.org/10.3390/batteries4020020).

- [52] C.R. Pals and J. Newman, "Thermal Modeling of the Lithium/Polymer Battery: II. Temperature Profiles in a Cell Stack," *J. Electrochem. Soc.*, vol. 142, pp. 3282–3288, 1995. doi: [10.1149/1.2049975](https://doi.org/10.1149/1.2049975).
- [53] Al S. Hallaj, H. Maleki, J.S. Hong, and J.R. Selman, "Thermal modeling and design considerations of lithium-ion batteries," *J. Power Sources*, vol. 83, pp. 1–8, 1999, doi: [10.1016/S0378-7753\(99\)00178-0](https://doi.org/10.1016/S0378-7753(99)00178-0).
- [54] K. Esfarjani, J. Garg, and G. Chen, "Modeling heat conduction from first principles," *Annu. Rev. Heat Transf.*, vol. 17, pp. 9–47, 2014, doi: [10.1615/AnnualRevHeatTransfer.2014007746](https://doi.org/10.1615/AnnualRevHeatTransfer.2014007746).
- [55] D.Y. Kim, B. Lee, M. Kim, and J.H. Moon, "Thermal assessment of lithium-ion battery pack system with heat pipe assisted passive cooling using Simulink," *Therm. Sci. Eng. Prog.*, vol. 46, p. 102230, 2023, doi: [10.1016/j.tsep.2023.102230](https://doi.org/10.1016/j.tsep.2023.102230).
- [56] J. Newman, "Temperature Rise in a Battery Module with Constant Heat Generation," *J. Electrochem. Soc.*, vol. 142, no. 4, p. 1054, 1995. doi: [10.1149/1.2044130](https://doi.org/10.1149/1.2044130).
- [57] S.C. Chen, C.C. Wan, and Y.Y. Wang, "Thermal analysis of lithium-ion batteries," *J. Power Sources*, vol. 140, pp. 111–124, 2005, doi: [10.1016/j.jpowsour.2004.05.064](https://doi.org/10.1016/j.jpowsour.2004.05.064).
- [58] W. Dreyer, J. Jamnik, C. Guhlke, R. Huth, J. Moškon, and M. Gaberšček, "The thermodynamic origin of hysteresis in insertion batteries," *Nat. Mater.*, vol. 9, pp. 448–453, 2010, doi: [10.1038/nmat2730](https://doi.org/10.1038/nmat2730).
- [59] Y. Li, Z. Zhou, and Wu. Wei-Tao "Three-Dimensional Thermal Modeling of Internal Shorting Process in a 20Ah Lithium-Ion Polymer Battery," *Energies*, vol. 13, no. 4, p. 1013, 2020, doi: [10.3390/en13041013](https://doi.org/10.3390/en13041013).
- [60] K. Thomas, J. Newman, and R. Darling, *Mathematical modeling of lithium batteries*, Kluwer Academic Publishers, Lawrence Berkeley National Laboratory, LBNL Report #: LBNL-53807, 2002. [Online] Available: <https://escholarship.org/uc/item/6905515d>.
- [61] W. Van Schalkwijk and B. Scrosati, "Advances in Lithium-Ion Batteries Introduction," in *Advances Lithium-Ion Batteries*, Springer New York, 2002, , pp. 1–5 doi: [10.1007/b113788](https://doi.org/10.1007/b113788).
- [62] K. Smith and C.-Y. Wang, "Power and thermal characterization of a lithium-ion battery pack for hybrid-electric vehicles," *J. Power Sources*, vol. 160, pp. 662–673, 2006, doi: [10.1016/j.jpowsour.2006.01.038](https://doi.org/10.1016/j.jpowsour.2006.01.038).
- [63] D.W. Sundin and S. Sponholtz, "Thermal Management of Li-Ion Batteries With Single-Phase Liquid Immersion Cooling," *IEEE Open J. Veh. Technol.*, vol. 1, pp. 82–92, 2020, doi: [10.1109/OJVT.2020.2972541](https://doi.org/10.1109/OJVT.2020.2972541).
- [64] W. Fang, O.J. Kwon, and C.-Y. Wang, "Electrochemical-thermal modeling of automotive Li-ion batteries and experimental validation using a three-electrode cell," *Int. J. Energy Res.*, vol. 34, pp. 107–115, 2009, doi: [10.1002/er.1652](https://doi.org/10.1002/er.1652).
- [65] U.S. Kim, J. Yi, C.B. Shin, T. Han, and S. Park, "Modeling the thermal behaviour of a lithium-ion battery during charge," *J. Power Sources*, vol. 196, pp. 5115–5121, 2011, doi: [10.1016/j.jpowsour.2011.01.103](https://doi.org/10.1016/j.jpowsour.2011.01.103).
- [66] R.E. Gerver and J.P. Meyers, "Three-Dimensional Modeling of Electrochemical Performance and Heat Generation of Lithium-Ion Batteries in Tabbed Planar Configurations," *J. Electrochem. Soc.*, vol. 158, no. 7, p. A835, 2011, doi: [10.1149/1.3591799](https://doi.org/10.1149/1.3591799).
- [67] J. Zhang, X.-G. Yang, F. Sun, Z. Wang, and C.-Y. Wang, "An online heat generation estimation method for lithium-ion batteries using dual-temperature measurements," *Appl. Energy*, vol. 272, p. 115262, 2020, doi: [10.1016/j.apenergy.2020.115262](https://doi.org/10.1016/j.apenergy.2020.115262).
- [68] P. Wang, L. Yang, H. Wang, D.M. Tartakovsky, and S. Onori, "Temperature estimation from current and voltage measurements in lithium-ion battery systems," *J. Energy Storage*, vol. 34, p.102133, 2021, doi: [10.1016/j.est.2020.102133](https://doi.org/10.1016/j.est.2020.102133).
- [69] S. Marelli and M. Corno, "Model-Based Estimation of Lithium Concentrations and Temperature in Batteries Using Soft-Constrained Dual Unscented Kalman Filtering," *IEEE Trans. Control Syst. Technol.*, vol. 29, no 2, pp. 926–933, 2021, doi: [10.1109/TCST.2020.2974176](https://doi.org/10.1109/TCST.2020.2974176).
- [70] X. Na, H. Kang, T. Wang, and Y. Wang, "Reverse layered air flow for Li-ion battery thermal management," *Appl. Therm. Eng.*, vol. 143, pp. 257–262, 2018, doi: [10.1016/j.applthermaleng.2018.07.080](https://doi.org/10.1016/j.applthermaleng.2018.07.080).
- [71] Ch. Park and A. Jaura, "Dynamic Thermal Model of Li-Ion Battery for Predictive Behavior in Hybrid and Fuel Cell Vehicles," *SAE Trans.*, vol. 112, pp. 1835–1842, 2023, doi: [10.4271/2003-01-2286](https://doi.org/10.4271/2003-01-2286).
- [72] D.J. Ravindra, R. Kumar, and L. Ma, "Thermal performance of a novel confined flow Li-ion battery module," *Appl. Therm. Eng.*, vol. 146, pp. 1–11, 2019, doi: [10.1016/j.applthermaleng.2018.09.099](https://doi.org/10.1016/j.applthermaleng.2018.09.099).
- [73] H. Maleki and A.K. Shamsuri, "Thermal analysis and modeling of a notebook computer battery," *J. Power Sources*, vol. 115 no. 1, pp. 131–136, 2003, doi: [10.1016/S0378-7753\(02\)00722-X](https://doi.org/10.1016/S0378-7753(02)00722-X).
- [74] X. Lin *et al.*, "A lumped-parameter electro-thermal model for cylindrical batteries," *J. Power Sources*, vol. 257, pp. 1–11, 2014, doi: [10.1016/j.jpowsour.2014.01.097](https://doi.org/10.1016/j.jpowsour.2014.01.097).
- [75] D. Li, and L. Yang, "Identification of spatial temperature gradient in large format lithium battery using a multilayer thermal model," *Int. J. Energy Res.*, vol. 44, no. 1, pp. 282–297, 2019, doi: [10.1002/er.4914](https://doi.org/10.1002/er.4914).
- [76] L. Xinfan, A.G. Stefanopoulou, H.E. Perez, J.B. Siegel, L. Yonghua, and R.D. Anderson, "Quadruple adaptive observer of the core temperature in cylindrical Li-ion batteries and their health monitoring," *2012 American Control Conference (ACC)*, 2012, doi: [10.1109/ACC.2012.6315386](https://doi.org/10.1109/ACC.2012.6315386).
- [77] X. Lin *et al.*, "Parameterization and Observability Analysis of Scalable Battery Clusters for Onboard Thermal Management," *Oil Gas Sci. Technol.*, vol. 68, no. 1, pp. 165–178, 2013, doi: [10.2516/ogst/2012075](https://doi.org/10.2516/ogst/2012075).
- [78] J. Sun *et al.*, "Online Internal Temperature Estimation for Lithium-Ion Batteries Based on Kalman Filter," *Energies*, vol. 8, no. 5, pp. 4400–4415, 2015, doi: [10.3390/en8054400](https://doi.org/10.3390/en8054400).
- [79] H. Dai, L. Zhu, J. Zhu, X. Wei, and Z. Sun, "Adaptive Kalman filtering based internal temperature estimation with an equivalent electrical network thermal model for hard-cased batteries," *J. Power Sources*, vol. 293, pp. 351–365, 2015, doi: [10.1016/j.jpowsour.2015.05.087](https://doi.org/10.1016/j.jpowsour.2015.05.087).
- [80] D.H. Doughty, P.C. Butler, R. Jungst, and E.P. Roth, "Lithium battery thermal models," *J. Power Sources*, vol. 110, pp. 357–363, 2002, doi: [10.1016/s0378-7753\(02\)00198-2](https://doi.org/10.1016/s0378-7753(02)00198-2).
- [81] Y. Zheng, Y. Che, X. Hu, X. Sui, D.-I. Stroe, and R. Teodorescu, "Thermal state monitoring of lithium-ion batteries: Progress, challenges, and opportunities," *Prog. Energy Combust. Sci.*, vol. 100, p. 101120, 2024, doi: [10.1016/j.pecs.2023.101120](https://doi.org/10.1016/j.pecs.2023.101120).

- [82] L. Sun, W. Sun, and F. You, "Core temperature modeling and monitoring of lithium-ion battery in the presence of sensor bias," *Appl. Energy*, vol. 271, p. 115243, 2020, doi: [10.1016/j.apenergy.2020.115243](https://doi.org/10.1016/j.apenergy.2020.115243).
- [83] C. Zhu, Y. Shang, F. Lu, Y. Jiang, C. Cheng, and C. Mi, "Core Temperature Estimation for Self-Heating Automotive Lithium-Ion Batteries in Cold Climates," *IEEE Trans. Ind. Inform.*, vol. 16, pp. 3366–3375, 2020, doi: [10.1109/TII.2019.2960833](https://doi.org/10.1109/TII.2019.2960833).
- [84] Y. Xiao, "Model-Based Virtual Thermal Sensors for Lithium-Ion Battery in EV Applications," *IEEE Trans. Ind. Electron.*, vol. 62, no. 5, pp. 3112–3122, 2015, doi: [10.1109/TIE.2014.2386793](https://doi.org/10.1109/TIE.2014.2386793).
- [85] Y. Ma, Y. Cui, H. Mou, J. Gao, and H. Chen, "Core Temperature Estimation of Lithium-Ion Battery for EVs Using Kalman Filter," *Appl. Therm. Eng.*, vol. 168, p. 114816, 2020, doi: [10.1016/j.applthermaleng.2019.114816](https://doi.org/10.1016/j.applthermaleng.2019.114816).
- [86] H. Ren, L. Jia, C. Dang, and Z. Qi, "An electrochemical-thermal coupling model for heat generation analysis of prismatic lithium battery," *J. Energy Storage*, vol. 50, p. 104277, 2022, doi: [10.1016/j.est.2022.104277](https://doi.org/10.1016/j.est.2022.104277).
- [87] D.H. Jeon, "Numerical modeling of lithium-ion battery for predicting thermal behavior in a cylindrical cell," *Curr. Appl. Phys.*, vol. 14, no. 2, pp. 196–205, 2014, doi: [10.1016/j.cap.2013.11.006](https://doi.org/10.1016/j.cap.2013.11.006).
- [88] N. Baba, H. Yoshida, M. Nagaoka, C. Okuda, and S. Kawachi, "Numerical simulation of thermal behavior of lithium-ion secondary batteries using the enhanced single particle model," *J. Power Sources*, vol. 252, pp. 214–228, 2014, doi: [10.1016/j.jpowsour.2013.11.111](https://doi.org/10.1016/j.jpowsour.2013.11.111).
- [89] S. Du *et al.*, "Study on the thermal behaviors of power lithium iron phosphate (LFP) aluminum-laminated battery with different tab configurations," *Int. J. Therm. Sci.*, vol. 89, pp. 327–336, 2015, doi: [10.1016/j.ijthermalsci.2014.11.018](https://doi.org/10.1016/j.ijthermalsci.2014.11.018).
- [90] J. Yi, J. Lee, C.B. Shin, T. Han, and S. Park, "Modeling of the transient behaviors of a lithium-ion battery during dynamic cycling," *J. Power Sources*, vol. 277, pp. 379–386, 2015, doi: [10.1016/j.jpowsour.2014.12.028](https://doi.org/10.1016/j.jpowsour.2014.12.028).
- [91] M. Fleckenstein, O. Bohlen, M.A. Roscher, and B. Bäker, "Current density and state of charge inhomogeneities in Li-ion battery cells with LiFePO₄ as cathode material due to temperature gradients," *J. Power Sources*, vol. 196, no. 10, pp. 4769–4778, 2011, doi: [10.1016/j.jpowsour.2011.01.043](https://doi.org/10.1016/j.jpowsour.2011.01.043).
- [92] R. Guo, L. Lu, M. Ouyang, and X. Feng, "Mechanism of the entire overdischarge process and overdischarge-induced internal short circuit in lithium-ion batteries," *Sci. Rep.*, vol. 6, no. 1, 2016, doi: [10.1038/srep30248](https://doi.org/10.1038/srep30248).
- [93] D. Rittel, "Transient temperature measurement using embedded thermocouples," *Exp. Mech.*, vol. 38, pp. 73–78, 1998, doi: [10.1007/BF02321647](https://doi.org/10.1007/BF02321647).
- [94] G. Zhang, S. Ge, T. Xu, X.G. Yang, H. Tian, and C.Y. Wang, "Rapid self-heating and internal temperature sensing of lithium-ion batteries at low temperatures," *Electrochim. Acta*, vol. 218, pp. 149–155, 2016, doi: [10.1016/j.electacta.2016.09.117](https://doi.org/10.1016/j.electacta.2016.09.117).
- [95] R. Srinivasan, B.G. Carkhuff, M.H. Butler, and A.C. Baisden, "Instantaneous measurement of the internal temperature in lithium-ion rechargeable cells," *Electrochim. Acta*, vol. 56, no. 17, pp. 6198–6204, 2011, doi: [10.1016/j.electacta.2011.03.136](https://doi.org/10.1016/j.electacta.2011.03.136).
- [96] R. Srinivasan, "Monitoring dynamic thermal behavior of the carbon anode in a lithium-ion cell using a four-probe technique," *J. Power Sources*, vol. 198, pp. 351–358, 2012, doi: [10.1016/j.jpowsour.2011.09.077](https://doi.org/10.1016/j.jpowsour.2011.09.077).
- [97] J.P. Schmidt, S. Arnold, A. Loges, D. Werner, T. Wetzel, E. Ivers-Tiffée, "Measurement of the internal cell temperature via impedance: Evaluation and application of a new method," *J. Power Sources*, vol. 243, pp. 110–117, 2013, doi: [10.1016/j.jpowsour.2013.06.013](https://doi.org/10.1016/j.jpowsour.2013.06.013).
- [98] Y. Troxler *et al.*, "The effect of thermal gradients on the performance of lithium-ion batteries," *J. Power Sources*, vol. 247, pp. 1018–1025, 2014, doi: [10.1016/j.jpowsour.2013.06.084](https://doi.org/10.1016/j.jpowsour.2013.06.084).
- [99] U. Tröltzsch, O. Kanoun, and H.-R. Tränkler, "Characterizing aging effects of lithium ion batteries by impedance spectroscopy," *Electrochim. Acta*, vol. 51, pp. 1664–1672, 2006, doi: [10.1016/j.electacta.2005.02.148](https://doi.org/10.1016/j.electacta.2005.02.148).
- [100] R.R. Richardson and D.A. Howey, "Sensorless Battery Internal Temperature Estimation Using a Kalman Filter With Impedance Measurement," *IEEE Trans. Sustain. Energy*, vol. 6, no. 4, pp. 1190–1199, 2015, doi: [10.1109/TSSTE.2015.2420375](https://doi.org/10.1109/TSSTE.2015.2420375).
- [101] J.G. Zhu, Z.C. Sun, X.Z. Wei, and H.F. Dai, "A new lithium-ion battery internal temperature on-line estimate method based on electrochemical impedance spectroscopy measurement," *J. Power Sources*, vol. 274, pp. 990–1004, 2015, doi: [10.1016/j.jpowsour.2014.10.182](https://doi.org/10.1016/j.jpowsour.2014.10.182).
- [102] M. Debert, G. Colin, G. Bloch, and Y. Chamailard, "An observer looks at the cell temperature in automotive battery packs," *Control Eng. Practice*, vol. 21, no. 8, pp. 1035–1042, 2013, doi: [10.1016/j.conengprac.2013.03.001](https://doi.org/10.1016/j.conengprac.2013.03.001).
- [103] X. Hu, H. Yuan, C. Zou, Z. Li, and L. Zhang, "Co-Estimation of State of Charge and State of Health for Lithium-Ion Batteries Based on Fractional-Order Calculus," *IEEE Trans. Veh. Technol.*, vol. 67, no. 11, pp. 10319–10329, 2018, doi: [10.1109/TVT.2018.2865664](https://doi.org/10.1109/TVT.2018.2865664).
- [104] Z. Wang, J. Ma, and L. Zhang, "State-of-Health Estimation for Lithium-Ion Batteries Based on the Multi-Island Genetic Algorithm and the Gaussian Process Regression," *IEEE Access*, vol. 5, pp. 21286–21295, 2017, doi: [10.1109/ACCESS.2017.2759094](https://doi.org/10.1109/ACCESS.2017.2759094).
- [105] A. Hande, "Internal battery temperature estimation using series battery resistance measurements during cold temperatures," *J. Power Sources*, vol. 158, no. 2, pp. 1039–1046, 2006, doi: [10.1016/j.jpowsour.2005.11.027](https://doi.org/10.1016/j.jpowsour.2005.11.027).
- [106] D.A. Howey, P.D. Mitcheson, V. Yufit, G.J. Offer, and N.P. Brandon, "Online Measurement of Battery Impedance Using Motor Controller Excitation," *IEEE Trans. Veh. Technol.*, vol. 63, no. 6, pp. 2557–2566, 2014, doi: [10.1109/TVT.2013.2293597](https://doi.org/10.1109/TVT.2013.2293597).
- [107] Z. Liu and H.-X. Li, "A Spatiotemporal Estimation Method for Temperature Distribution in Lithium-Ion Batteries," *IEEE Trans. Ind. Inform.*, vol. 10, no. 4, pp. 2300–2307, 2014, doi: [10.1109/TII.2014.2341955](https://doi.org/10.1109/TII.2014.2341955).
- [108] R. Khelif, Chebel-B. Morello, S. Malinowski, E. Laajili, F. Fnaiech, and N. Zerhouni, "Direct Remaining Useful Life Estimation Based on Support Vector Regression," *IEEE Trans. Ind. Electron.*, vol. 64, no. 3, pp. 2276–2285, 2017, doi: [10.1109/TIE.2016.2623260](https://doi.org/10.1109/TIE.2016.2623260).
- [109] C. Sbarufatti, M. Corbetta, M. Giglio, and F. Cadini, "Adaptive prognosis of lithium-ion batteries based on the combination of particle filters and radial basis function neural networks," *J. Power Sources*, vol. 344, pp. 128–140, 2017, doi: [10.1016/j.jpowsour.2017.01.105](https://doi.org/10.1016/j.jpowsour.2017.01.105).

- [110] K. Liu, K. Li, Q. Peng, Y. Guo, and L. Zhang, "Data-Driven Hybrid Internal Temperature Estimation Approach for Battery Thermal Management," *Complexity*, vol. 2018, p. 9642892, 2018, doi: [10.1155/2018/9642892](https://doi.org/10.1155/2018/9642892).
- [111] F. Feng *et al.*, "Co-estimation of lithium-ion battery state of charge and state of temperature based on a hybrid electrochemical-thermal-neural-network model," *J. Power Sources*, vol. 455, p. 227935, 2020, doi: [10.1016/j.jpowsour.2020.22.7935](https://doi.org/10.1016/j.jpowsour.2020.22.7935).
- [112] Y. Li, W. Liu, and J. Zhong, "Comparison of noninvasive and remote temperature estimation employing magnetic nanoparticles in DC and AC applied fields," *2012 IEEE International Instrumentation and Measurement Technology Conference Proceedings*, 2012, doi: [10.1109/I2MTC.2012.6229437](https://doi.org/10.1109/I2MTC.2012.6229437).
- [113] J. Zhong, J. Dieckhoff, M. Schilling, and F. Ludwig, "Influence of static magnetic field strength on the temperature resolution of a magnetic nanoparticle thermometer," *J. Appl. Phys.*, vol. 120, no. 14, p. 143902, 2016, doi: [10.1063/1.4964696](https://doi.org/10.1063/1.4964696).
- [114] J. Zhong, W. Liu, Z. Du, C.P. Morais, Q. Xiang, and Q. Xie, "A noninvasive, remote and precise method for temperature and concentration estimation using magnetic nanoparticles," *Nanotechnology*, vol. 23, no. 7, p. 075703, 2012, doi: [10.1088/0957-4484/23/7/075703](https://doi.org/10.1088/0957-4484/23/7/075703).
- [115] Y. Ma, Y. Cui, H. Mou, J. Gao, and H. Chen, "Core temperature estimation of lithium-ion battery for EVs using Kalman filter," *Appl. Therm. Eng.*, vol. 168, p. 114816, 2020, doi: [10.1016/j.applthermaleng.2019.114816](https://doi.org/10.1016/j.applthermaleng.2019.114816).